GEOLOGY | THE GEOLOGICAL SOCIETY OF AMERICA®

https://doi.org/10.1130/G46274.1

Manuscript received 13 December 2018
Revised manuscript received 4 July 2019
Manuscript accepted 10 July 2019

Published online 12 August 2019

Moderate levels of Eocene pCO_2 indicated by Southern Hemisphere fossil plant stomata

Margret Steinthorsdottir[1,2*], Vivi Vajda[1], Mike Pole[3], and Guy Holdgate[4]

[1]Department of Palaeobiology, Swedish Museum of Natural History, SE 104 05 Stockholm, Sweden
[2]Bolin Centre for Climate Research, Stockholm University, SE 109 61 Stockholm, Sweden
[3]Queensland Herbarium, Brisbane Botanic Gardens, Mount Coot-tha Road, Toowong, Queensland 4066, Australia
[4]School of Earth Sciences, University of Melbourne, Parkville, Victoria 3010, Australia

ABSTRACT

Reducing the uncertainty in predictions of future climate change is one of today's greatest scientific challenges, with many significant problems unsolved, including the relationship between pCO_2 and global temperature. To better constrain these forecasts, it is meaningful to study past time intervals of global warmth, such as the Eocene (56.0–33.9 Ma), serving as climatic analogues for the future. Here we reconstructed pCO_2 using the stomatal densities of a large fossil Lauraceae (laurel) leaf database from ten sites across the Eocene of Australia and New Zealand. We show that mostly moderate pCO_2 levels of ~450–600 ppm prevailed throughout the Eocene, levels that are considerably lower than the pCO_2 forcing currently needed to recreate Eocene temperatures in climate models. Our data record significantly lower pCO_2 than inferred from marine isotopes, but concur with previously published Northern Hemisphere Eocene stomatal proxy pCO_2. We argue that the now globally consistent stomatal proxy pCO_2 record for the Eocene is robust and that climate sensitivity was elevated and/or that additional climate forcings operated more powerfully than previously assumed.

INTRODUCTION

The anthropogenic rise in CO_2 concentrations (pCO_2) is predicted to result in a global average temperature increase of up to 4 °C by the year 2100 (IPCC, 2014), with severe socioeconomic and ecosystem impacts predicted. However, the exact relationship between pCO_2 and temperature—or climate sensitivity (the equilibrium response in mean global surface temperatures to a doubling of pCO_2, generally reported as ~3 °C)—is still not well understood, and is probably state-dependent; i.e., dependent on baseline pCO_2 and temperature. Scientists therefore look to past time intervals of global warming, which can serve as "climatic analogues", for clues about our future. The Eocene epoch was such a time interval, with average global temperatures 4–15 °C higher than at present (Zachos et al., 2001; Huber and Caballero, 2011; Anagnostou et al., 2016; Cramwinckel et al., 2018). In the earliest Eocene (ca. 55.5 Ma), there was a transient episode of extremely elevated temperatures—the Paleocene-Eocene Thermal Maximum, or PETM (McInerney and Wing, 2011). Later, after the peak warmth of the Early Eocene Climatic Optimum (EECO, ca. 52–50 Ma), a gradual cooling began, briefly interrupted by a major warming reversal at ca. 40 Ma, called the Middle Eocene Climatic Optimum (MECO) (Zachos et al., 2001; Cramwinckel et al., 2018). The Eocene climate still constitutes one of the greatest unsolved problems in paleoclimate research. Temperatures were globally much higher than today, with a significantly weaker equator-to-pole temperature gradient and a muted seasonal cycle compared to today, referred to as the "Eocene equable climate problem" (Sloan and Barron, 1990; Greenwood and Wing, 1995; Greenwood et al., 2003a). Climate modeling has been able to reconstruct this pattern with very high pCO_2 levels (up to ~4500 ppm: Huber and Caballero, 2011), but such extremely elevated pCO_2 is not documented by proxy records. It is therefore assumed that Eocene climate sensitivity—often defined as Earth system sensitivity for longer time scales, including both "fast" and "slow" feedbacks (Lunt et al., 2010)—was elevated compared to present, and/or that other mechanisms, in addition to the dominant forcing of pCO_2, were in operation (Caballero and Huber, 2013; Anagnostou et al., 2016; Zeebe et al., 2016; Carlson and Caballero, 2016; Cramwinckel et al., 2018; Keery et al., 2018). A variety of geochemical and biological proxies as well as carbon cycle modeling have been used to estimate Eocene pCO_2, but these estimates still differ hugely (with values ranging from hundreds to thousands of parts per million pCO_2); however, there is some convergence forming (Holdgate et al., 2009; Beerling and Royer, 2011; Foster et al., 2017). To further constrain Eocene pCO_2, additional proxy records of sufficient quality and resolution are urgently required. Here, we contribute to this quest by presenting a new terrestrial record of Eocene pCO_2 using a stomatal proxy method of paleo-pCO_2 reconstruction.

MATERIAL AND METHODS

We photographed and analyzed 92 fossil Lauraceae (angiosperm) specimens from six Australian and four New Zealand localities (Fig. 1), derived from ten relatively well-dated stratigraphic levels spanning the Eocene. The database of specimens consists of permanently mounted cuticle samples on microscope slides, prepared in connection with previous taxonomic work, following standard paleobotanical procedures. The database derives from two separate collections, with 46 specimens hosted at Melbourne Museum, Melbourne, Victoria, Australia, and the remaining 46 at the School of Environment, University of Auckland, New Zealand (see Appendix DR1 in the

*E-mail: margret.steinthorsdottir@nrm.se

CITATION: Steinthorsdottir, M., Vajda, V., Pole, M., and Holdgate, G., 2019, Moderate levels of Eocene *p*CO2 indicated by Southern Hemisphere fossil plant stomata: Geology, v. 47, p. 914–918, https://doi.org/10.1130/G46274.1

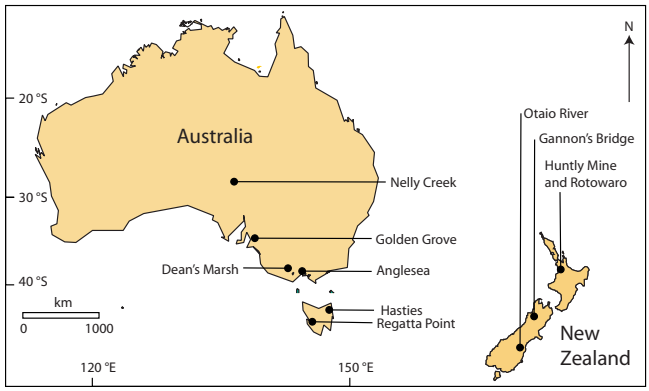

Figure 1. Location of field sites in Australia and New Zealand from where Lauraceae (laurel) leaf cuticle specimens were collected.

GSA Data Repository[1] for details). We reconstructed paleo-pCO_2 using the stomatal proxy, founded on the observed inverse relationship between the density of leaf stomata and pCO_2 (Woodward, 1987; McElwain and Steinthorsdottir, 2017). Stomatal density of plant leaves was quantified from microscope images as stomatal index (SI [%] = proportion of stomata relative to all epidermal cells). Three methods of stomatal proxy paleo-pCO_2 reconstructions are currently in use:

1. The semiquantitative empirical stomatal ratio method, which utilizes the ratio between the SI of fossil plants and the SI of extant nearest living relatives or equivalents (NLRs or NLEs), grown in known pCO_2 (living or herbaria specimens), to estimate paleo-pCO_2 (McElwain, 1998);
2. The also empirical transfer function method, which uses herbarium and/or experimental data sets of NLR-NLE responses to variations in pCO_2 to construct regression curves on which fossil SI can be plotted to infer paleo-pCO_2 (e.g., Barclay and Wing, 2016);
3. Mechanistic gas exchange modeling, which is taxon-independent (relying on morphological measurement data), but also requires input of additional parameters, such as leaf $\delta^{13}C$ and paleotemperature (Konrad et al., 2008; Franks et al., 2014; Konrad et al., 2017).

Here the Lauraceae database is without leaf $\delta^{13}C$ data, so we used the stomatal ratio and transfer function methods to reconstruct Eocene pCO_2, employing multiple NLEs to minimize interspecies variation and reach best-consensus pCO_2. The NLE species used in the stomatal ratio method were *Litsea glutinosa* (Indian laurel), *L. fuscata*, *L. stocksii, Neolitsea dealbata* (bolly gum), and *Cinnamomum camphora* (camphor laurel), and *Laurus nobilis* (bay laurel) was used in the transfer function (from Kürschner et al. [2008], including the recommended correction factor of + 150 ppm), using the equations:

$$\text{Stomatal ratio: } pCO_{2\,\text{paleo}} = SI_{NLE} / SI_{fossil} \times pCO_{2\,\text{modern}}, \quad (1)$$

$$\text{Transfer function: } pCO_{2\,\text{paleo}} = 10^{3.173} - \left[0.5499 \times \log\left(SI_{fossil}\right)\right] + 150. \quad (2)$$

(For details on the stomatal proxy pCO_2 reconstruction, stratigraphic setting, and chronology, see Appendix DR1, including Figs. DR1 and DR2, and data set Appendix DR2 in the Data Repository).

RESULTS AND DISCUSSION

Southern Hemisphere Stomatal Proxy pCO_2 Reconstruction

Early Eocene (ca. 54–50 Ma) Lauraceae leaf cuticles from the Otaio River (South Island, New Zealand) and Regatta Point (Tasmania) record SIs of 11.5% and 11.2%, respectively, and those from Dean's Marsh (southern Australia), 13.4% (Table 1). The early Eocene SIs translate into average pCO_2 of ~520–540 ppm and ~450 ppm, respectively (Fig. 2, pink dots). These results are highly comparable to previously published stomatal proxy pCO_2 estimates (Fig. 2, green diamonds), but much lower than contemporaneous marine boron isotope pCO_2 (white square) and, together with these, capture rising pCO_2 and temperatures into the EECO. The next cluster of Lauraceae cuticles, from the middle Eocene (ca. 45–39 Ma), show SI values of 12% and 14.6% at the broadly contemporaneous Nelly Creek and Golden Grove localities (Australia), and 10.4% at the slightly younger Hasties locality (Tasmania) (Table 1). These indicate pCO_2 of ~430–490 ppm and ~590 ppm, respectively (Fig. 2). These results are broadly comparable with previously published stomatal estimates, but lower than marine pCO_2, together indicating rising pCO_2 and temperatures into the MECO (Fig. 2). Earliest late Eocene (ca. 38 Ma) Lauraceae show SI values of 11.4% and 11% at Gannon's Bridge (South Island, New Zealand) and Rotowaro (North Island, New Zealand) and 12.1% at Anglesea (Australia), translating to pCO_2 of 510–550 ppm (Table 1; Fig. 2), in full agreement with previously published stomatal pCO_2 estimates, but lower than most of the marine isotope pCO_2 records (white and black squares). We also calibrated earliest late Eocene pCO_2 using several specimens of *Cinnamomum* sp. from the Anglesea locality, resulting in a much higher pCO_2 at ~725 ppm. This could indicate that the more generalized Lauraceae specimen database underestimates pCO_2, but given the near-identical lower pCO_2 estimates from three separate localities in this study and from well-dated contemporaneous *Metasequoia* (redwood) needles (Doria et al., 2011), this seems unlikely. Finally, in the later late Eocene (ca. 35 Ma), we record a SI from Huntly Mine (North Island, New Zealand) at 7.7%, translating to pCO_2 of ~750 ppm (Table 1; Fig. 2). These results are based however on only two specimens, and should not be considered robust. We note nonetheless that the high estimate agrees with previously published coeval stomatal pCO_2 results (Roth-Nebelsick et al., 2012), as well as with the lower range of marine isotope–based pCO_2 estimates (Fig. 2).

Note that error bars on the *y*-axis in Figure 2 show the standard deviation for the pCO_2 estimates, not including uncertainties in the calibration regressions. The full error range of stomatal-derived pCO_2 is difficult to quantify, but has been estimated in some cases to be up to 200% and right skewed (larger error at higher pCO_2) for the stomatal index and transfer function methods (Beerling et al., 2009; Foster et al., 2017). Error bars on the *x*-axis show the full likely chronological range of each sample locality (see also Fig. DR1).

Comparison to Existing pCO_2 Records and Implications

The Eocene pCO_2 results obtained using Southern Hemisphere Lauraceae mostly fall in the relatively moderate interval of ~450–600 ppm, which is highly comparable to previously published coeval stomatal proxy records (Fig. 2), but lower than marine records, which mostly record pCO_2 of ~800–1400 ppm (Pearson et al., 2009; Zhang et al., 2013; Anagnostou et al., 2016; Fig. 2), whereas existing paleosol records form less internal consensus, recording ~80–1300 ppm, and mostly derive from the narrow time interval 54–52 Ma (Foster et al., 2017). Due to the generally poorer stratigraphic and chronologic control of terrestrial sedimentary sections relative to marine records, it is challenging to directly correlate our results with the marine pCO_2 and temperature records. However, the stomatal proxy pCO_2 record captures some of the major changes in pCO_2 during the principal

[1]GSA Data Repository item 2019329, geological background and chronology, details on stomatal proxy paleo-pCO_2 reconstruction (Appendix DR1, including supplementary Figs. DR1–DR2), and full data set (Appendix DR2), is available online at http://www.geosociety.org/datarepository/2019/, or on request from editing@geosociety.org.

TABLE 1. EOCENE STOMATAL INDICES AND PCO_2 RECONSTRUCTION, AUSTRALIA AND NEW ZEALAND

Locality	Age (Ma)	Average SI (%)	pCO_2, stomatal ratio method (ppm)					pCO_2, transfer function (ppm)	Average pCO_2 (ppm)
			Litsea glutinosa	*Litsea fuscata*	*Litsea stocksii*	*Neolitsea dealbata*	*Cinnamomum camphora*	*Laurus nobilis*	
Huntly Mine, NZ	34.5–37	**7.7** ± 0.95	902 ± 118	869 ± 114	684 ± 90	669 ± 88		638 ± 35	**752** ± 123
Anglesea, AUS	38 ± 1	**12.1** ± 1.5	583 ± 97	562 ± 93	442 ± 74	435 ± 72		533 ± 35	**511** ± 67
		8.9 ± 1.1					723 ± 89		**723** ± 89
Rotowaro, NZ	36.5–39	**11.0** ± 0.15	638 ± 116	614 ± 112	483 ± 88	473 ± 86		553 ± 40	**552** ± 75
Gannon's Bridge, NZ	37–39	**11.4** ± 1.0	606 ± 53	583 ± 52	459 ± 41	449 ± 40		542 ± 19	**528** ± 71
Hasties, AUS	40–42	**10.4** ± 2.4	689 ± 150	663 ± 145	522 ± 114	511 ± 111		569 ± 51	**591** ± 81
Golden Grove, AUS	39–45	**14.6** ± 1.5	480 ± 47	462 ± 45	364 ± 36	358 ± 35		495 ± 19	**432** ± 66
Nelly Creek, AUS	39–45	**12.0** ± 12	573 ± 1.0	552 ± 48	382 ± 47	427 ± 68		531 ± 36	**493** ± 84
Dean's Marsh, AUS	52–53	**13.4** ± 2.4	515 ± 54	496 ± 52	325 ± 34	384 ± 40		509 ± 21	**446** ± 86
Regatta Point, AUS	48.5–55	**11.5** ± 1.0	600 ± 60	578 ± 58	455 ± 45	445 ± 44		540 ± 21	**523** ± 71
Otaio River, NZ	51–56	**11.2** ± 1.4	619 ± 79	596 ± 76	469 ± 60	459 ± 59		547 ± 28	**538** ± 73

Note: NZ—New Zealand; AUS—Australia (see Figure 1 for map of localities). Average stomatal indices (SI) of Lauraceae leaves are reported from each locality. Calibrated pCO_2 estimates are based on five nearest living equivalents (NLEs) in the stomatal ratio method and one NLE via a transfer function, with overall average pCO_2 listed in bold in the final right column. All values are listed with standard deviation. For the full data set, see Appendix DR2 (see text footnote 1).

climatic events of the Eocene recorded by the deep ocean–derived temperature record, such as rising pCO_2 at the transition into the EECO or MECO (Fig. 2).

The most striking feature of the Eocene stomatal proxy record is that some of the highest pCO_2 is indicated in the early middle Eocene (until ca. 46–44 Ma), well beyond the end of the EECO, in reasonable agreement with the couple of marine isotope data points in this interval, whereas the deep-ocean proxy compilation tracks a gradual temperature decline between the EECO and MECO (Fig. 2). After ca. 46–44 Ma, a decrease in stomatal pCO_2 is recorded prior to the MECO, followed by a moderate increase at the transition into the MECO (Fig. 2). These trends do not fully agree with the deep-ocean compilation, but it should be noted that terrestrial mean annual temperature (MAT) records suggest a correlation between stomatal-recorded pCO_2 and MAT during this time (e.g., Greenwood et al., 2003a; Pancost et al., 2013). In the later part of the late Eocene, stomatal and marine isotope records show a fairly high range in coeval pCO_2 values, with the stomatal record displaying a closer congruence with the deep-ocean compilation temperature than the marine pCO_2 record (Fig. 2).

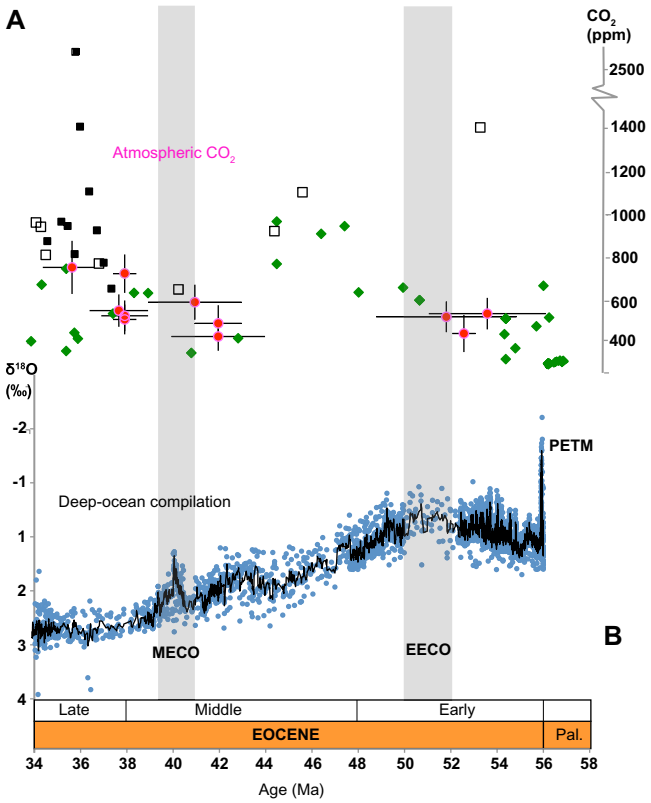

Figure 2. Eocene climate reconstructions. (A) Green diamonds show previously published stomatal proxy–derived pCO_2 estimates for the Eocene (McElwain, 1998; Kürschner et al., 2001; Royer et al., 2001; Greenwood et al., 2003b; Retallack, 2009; Smith et al., 2010; Doria et al., 2011; Grein et al., 2011; Roth-Nebelsick et al., 2012; Franks et al., 2014; Maxbauer et al., 2014; Liu et al., 2016; Steinthorsdottir et al., 2016; Wolfe et al., 2017). Pink circles are average pCO_2 values calibrated in the present study. Marine pCO_2 estimates based on alkenone $\delta^{13}C$ data are shown with black squares (Zhang et al., 2013), while white squares are based on boron $\delta^{11}B$ data (Pearson et al., 2009; Anagnostou et al., 2016). All previously published data points are plotted without errors for visual clarity; see Foster et al. (2017) for error estimates. (B) $\delta^{18}O$-based ice-free deep-ocean temperature proxy (lower values indicate higher temperatures), with five-point running average curve fitted in black (data compilation of Cramwinckel et al., 2018). PETM—Paleocene-Eocene Thermal Maximum; EECO—Early Eocene Climatic Optimum; MECO—Middle Eocene Climatic Optimum; Pal.—Paleocene.

Stomatal proxy pCO_2 reconstructions currently offer the highest-resolution record of Eocene pCO_2, with almost 50 data points, compared to ~10 each derived from marine alkenone and boron isotopes, and ~20 from paleosols. The numerous studies, using various fossil angiosperms as well as the fossil gymnosperms *Ginkgo* and *Metasequoia*, in the three stomatal proxy methods currently in use mostly agree that the Eocene pCO_2 was more moderately elevated compared to what marine proxies and climate modeling suggest (McElwain, 1998; Kürschner et al., 2001; Royer et al., 2001; Greenwood et al., 2003b; Retallack, 2009; Smith et al., 2010; Doria et al., 2011; Grein et al., 2011; Roth-Nebelsick et al., 2012; Franks et al., 2014; Maxbauer et al., 2014; Liu et al., 2016; Steinthorsdottir et al., 2016; Wolfe et al., 2017). The discrepancy between the marine isotope and stomatal proxy pCO_2 results is considerable, with the marine isotopes recording pCO_2 currently assumed to be more consistent with the elevated Eocene temperatures recorded by numerous proxies and the workings of the Earth's climate system (Cramwinckel et al., 2018). Our results provide new SI data from the previously sparse Southern Hemisphere record, suggesting that the terrestrial pCO_2 proxy data may indeed be robust with an internally consistent global record of moderate Eocene pCO_2 levels. Although it is premature to make strong statements, this would imply that Earth system sensitivity was likely in the range of ~4–8 °C during the Eocene, significantly elevated compared to the "modern" climate sensitivity of ~3 °C (Lunt et al., 2010; Royer et al., 2012; Maxbauer et al., 2014; Wolfe et al., 2017; Keery et al., 2018; Schneider et al., 2019). However, the various feedback mechanisms affecting Earth system sensitivity in an ice-free world are still poorly understood.

In summary, we find pCO_2 of ~450–600 ppm recorded by Southern Hemisphere fossil plants throughout the Eocene—significantly less than the forcing required by modeling, suggesting that climate sensitivity was elevated and/or that other climate forcings were stronger than previously assumed.

ACKNOWLEDGMENTS

Melbourne Museum (Victoria, Australia) is gratefully acknowledged for access to the late Dr. David Christophel's leaf cuticle collection. We thank Matthew Huber and David Greenwood for valuable discussions and suggestions on an earlier draft of this paper. Funding from the Swedish Research Council (VR Starting Grant NT-7 2016 04905 to Steinthorsdottir, and VR 2015 4264 to Vajda), and from the Bolin Centre for Climate Research, Stockholm University, to Steinthorsdottir is gratefully acknowledged. Three anonymous reviewers provided valuable feedback on the manuscript.

REFERENCES CITED

Anagnostou, E., John, E.H., Edgar, K.M., Foster, G.L., Ridgwell, A., Inglis, G.N., Pancost, R.D., Lunt, D.J., and Pearson, P.N., 2016, Changing atmospheric CO_2 concentration was the primary driver of early Cenozoic climate: Nature, v. 533, p. 380–384, https://doi.org/10.1038/nature17423.

Barclay, R.S., and Wing, S.L., 2016, Improving the Ginkgo CO_2 barometer: Implications for the early Cenozoic atmosphere: Earth and Planetary Science Letters, v. 439, p. 158–171, https://doi.org/10.1016/j.epsl.2016.01.012.

Beerling, D.J., and Royer, D.L., 2011, Convergent Cenozoic CO_2 history: Nature Geoscience, v. 4, p. 418–420, https://doi.org/10.1038/ngeo1186.

Beerling, D.J., Fox, A., and Anderson, C.W., 2009, Quantitative uncertainty analyses of ancient atmospheric CO_2 estimates from fossil leaves: American Journal of Science, v. 309, p. 775–787, https://doi.org/10.2475/09.2009.01.

Caballero, R., and Huber, M., 2013, State-dependent climate sensitivity in past warm climates and its implications for future climate projections: Proceedings of the National Academy of Sciences of the United States of America, v. 110, p. 14,162–14,167, https://doi.org/10.1073/pnas.1303365110.

Carlson, H., and Caballero, R., 2016, Atmospheric circulation and hydroclimate impacts of alternative warming scenarios for the Eocene: Climate of the Past, v. 13, p. 1037–1048, https://doi.org/10.5194/cp-13-1037-2017.

Cramwinckel, M.J., et al., 2018, Synchronous tropical and polar temperature evolution in the Eocene: Nature, v. 559, p. 382–386, https://doi.org/10.1038/s41586-018-0272-2.

Doria, G., Royer, D.L., Wolfe, A.P., Fox, A., Westgate, J.A., and Beerling, D.J., 2011, Declining atmospheric CO_2 during the late Middle Eocene climate transition: American Journal of Science, v. 311, p. 63–75, https://doi.org/10.2475/01.2011.03.

Foster, G.L., Royer, D.L., and Lunt, D.J., 2017, Future climate forcing potentially without precedent in the last 420 million years: Nature Communications, v. 8, 14845, https://doi.org/10.1038/ncomms14845.

Franks, P.J., Royer, D.L., Beerling, D.J., Van de Water, P.K., Cantrill, D.J., Barbour, M.M., and Berry, J.A., 2014, New constraints on atmospheric CO_2 concentration for the Phanerozoic: Geophysical Research Letters, v. 41, p. 4685–4694, https://doi.org/10.1002/2014GL060457.

Greenwood, D.R., and Wing, S.L., 1995, Eocene continental climates and latitudinal temperature gradients: Geology, v. 23, p. 1044–1048, https://doi.org/10.1130/0091-7613(1995)023<1044:ECCALT>2.3.CO;2.

Greenwood, D.R., Moss, P.T., Rowett, A.I., Vadala, A.J., and Keefe, R.L., 2003a, Plant communities and climate change in southeastern Australia during the early Paleogene, *in* Wing, S.I., et al., eds., Causes and Consequences of Globally Warm Climates in the Early Paleogene: Geological Society of America Special Paper 369, p. 365–380, https://doi.org/10.1130/0-8137-2369-8.365.

Greenwood, D.R., Scarr, M.J., and Christophel, D.C., 2003b, Leaf stomatal frequency in the Australian tropical rainforest tree *Neolitsea dealbata* (Lauraceae) as a proxy measure of atmospheric pCO_2: Palaeogeography, Palaeoclimatology, Palaeoecology, v. 196, p. 375–393, https://doi.org/10.1016/S0031-0182(03)00465-6.

Grein, M., Konrad, W., Wilde, V., Utescher, T., and Roth-Nebelsick, A., 2011, Reconstruction of atmospheric CO_2 during the early middle Eocene by application of a gas exchange model to fossil plants from the Messel Formation, Germany: Palaeogeography, Palaeoclimatology, Palaeoecology, v. 309, p. 383–391, https://doi.org/10.1016/j.palaeo.2011.07.008.

Holdgate, G.R., McGowran, B., Fromhold, T., Wagstaff, B.E., Gallagher, S.J., Wallace, M.W., Sluiter, I.R.K., and Whitelaw, M., 2009, Eocene–Miocene carbon isotope and floral record from brown coal seams in the Gippsland Basin of southeast Australia: Global and Planetary Change, v. 65, p. 89–103, https://doi.org/10.1016/j.gloplacha.2008.11.001.

Huber, M., and Caballero, R., 2011, The early Eocene equable climate problem revisited: Climate of the Past, v. 7, p. 603–633, https://doi.org/10.5194/cp-7-603-2011.

IPCC (Intergovernmental Panel on Climate Change), 2014, Climate Change 2014: Synthesis Report: Contribution of Working Groups I, II and III to the Fifth Assessment Report of the Intergovernmental Panel on Climate Change: Geneva, Switzerland, IPCC, 151 p.

Keery, J.S., Holden, P.B., and Edwards, N.R., 2018, Sensitivity of Eocene climate to CO_2 and orbital variability: Climate of the Past, v. 14, p. 215–238, https://doi.org/10.5194/cp-14-215-2018.

Konrad, W., Roth-Nebelsick, A., and Grein, M., 2008, Modelling of stomatal density response to atmospheric CO_2: Journal of Theoretical Biology, v. 253, p. 638–658, https://doi.org/10.1016/j.jtbi.2008.03.032.

Konrad, W., Katul, G., Roth-Nebelsick, A., and Grein, M., 2017, A reduced order model to analytically infer atmospheric CO_2 concentration from stomatal and climate data: Advances in Water Resources, v. 104, p. 145–157, https://doi.org/10.1016/j.advwatres.2017.03.018.

Kürschner, W.M., Wagner, F., Dilcher, D.L., and Visscher, H., 2001, Using fossil leaves for the reconstruction of Cenozoic paleoatmospheric CO_2 concentrations, *in* Gerhard, L.C., et al., eds., Geological Perspectives of Global Climate Change: American Association of Petroleum Geologists Studies in Geology 47, p. 169–189.

Kürschner, W.M., Kvaček, Z., and Dilcher, D.L., 2008, The impact of Miocene atmospheric carbon dioxide fluctuations on climate and the evolution of terrestrial ecosystems: Proceedings of the National Academy of Sciences of the United States of America, v. 105, p. 449–453, https://doi.org/10.1073/pnas.0708588105.

Liu, X.Y., Gao, Q., Han, M., and Jin, J.H., 2016, Estimates of late middle Eocene pCO_2 based on stomatal density of modern and fossil *Nageia* leaves: Climate of the Past, v. 12, p. 241–253, https://doi.org/10.5194/cp-12-241-2016.

Lunt, D.J., Haywood, A.M., Schmidt, G.A., Salzmann, U., Valdes, P.J., and Dowsett, H.J., 2010, Earth system sensitivity inferred from Pliocene modelling and data: Nature Geoscience, v. 3, p. 60–64, https://doi.org/10.1038/ngeo706.

Maxbauer, D.P., Royer, D.L., and LePage, B.A., 2014, High Arctic forests during the middle Eocene supported by moderate levels of atmospheric CO_2: Geology, v. 42, p. 1027–1030, https://doi.org/10.1130/G36014.1.

McElwain, J.C., 1998, Do fossil plants signal palaeoatmospheric carbon dioxide concentration in the geological past?: Philosophical Transactions of the Royal Society of London: Series B, Biological Sciences, v. 353, p. 83–96, https://doi.org/10.1098/rstb.1998.0193.

McElwain, J.C., and Steinthorsdottir, M., 2017, Paleoecology, ploidy, paleoatmospheric composition, and developmental biology: A review of the multiple uses of fossil stomata: Plant Physiology, v. 174, p. 650–664, https://doi.org/10.1104/pp.17.00204.

McInerney, F.A., and Wing, S.L., 2011, The Paleocene-Eocene Thermal Maximum: A perturbation of carbon cycle, climate, and biosphere with implications for the future: Annual Review of Earth and Planetary Sciences, v. 39, p. 489–516, https://doi.org/10.1146/annurev-earth-040610-133431.

Pancost, R.D., et al., 2013, Early Paleogene evolution of terrestrial climate in the SW Pacific, southern New Zealand: Geochemistry Geophysics Geosystems, v. 14, p. 5413–5429, https://doi.org/10.1002/2013GC004935.

Pearson, P.N., Foster, G.L., and Wade, B.S., 2009, Atmospheric carbon dioxide through the Eocene–Oligocene climate transition: Nature, v. 461, p. 1110–1113, https://doi.org/10.1038/nature08447.

Retallack, G.J., 2009, Greenhouse crises of the past 300 million years: Geological Society of America Bulletin, v. 121, p. 1441–1455, https://doi.org/10.1130/B26341.1.

Roth-Nebelsick, A., Grein, M., Utescher, T., and Konrad, W., 2012, Stomatal pore length change in leaves of *Eotrigonobalanus furcinervis* (Fagaceae) from the Late Eocene to the Latest Oligocene and its impact on gas exchange: Review of Palaeobotany and Palynology, v. 174, p. 106–112, https://doi.org/10.1016/j.revpalbo.2012.01.001.

Royer, D.L., Wing, S.L., Beerling, D.J., Jolley, D.W., Koch, P.L., Hickey, L.J., and Berner, R.A., 2001, Paleobotanical evidence for near present-day levels of atmospheric CO2 during part of the Tertiary: Science, v. 292, p. 2310–2313, https://doi.org/10.1126/science.292.5525.2310.

Royer, D.L., Pagani, M., and Beerling, D.J., 2012, Geobiological constraints on Earth system sensitivity to CO2 during the Cretaceous and Cenozoic: Geobiology, v. 10, p. 298–310, https://doi.org/10.1111/j.1472-4669.2012.00320.x.

Schneider, T., Kaul, C.M., and Pressel, K.G., 2019, Possible climate transitions from breakup of stratocumulus decks under greenhouse warming: Nature Geoscience, v. 12, p. 163–167, https://doi.org/10.1038/s41561-019-0310-1.

Sloan, L.C., and Barron, E.J., 1990, "Equable" climates during Earth history?: Geology, v. 18, p. 489–492, https://doi.org/10.1130/0091-7613(1990)018<0489:ECDEH>2.3.CO;2.

Smith, R.Y., Greenwood, D.R., and Basinger, J.F., 2010, Estimating paleoatmospheric pCO_2 during the Early Eocene Climatic Optimum from stomatal frequency of *Ginkgo*, Okanagan Highlands, British Columbia, Canada: Palaeogeography, Palaeoclimatology, Palaeoecology, v. 293, p. 120–131, https://doi.org/10.1016/j.palaeo.2010.05.006.

Steinthorsdottir, M., Porter, A.S., Holohan, A., Kunzmann, L., Collinson, M., and McElwain, J.C., 2016, Fossil plant stomata indicate decreasing atmospheric CO_2 prior to the Eocene-Oligocene boundary: Climate of the Past, v. 12, p. 439–454, https://doi.org/10.5194/cp-12-439-2016.

Wolfe, A.P., Reyes, A.V., Royer, D.L., Greenwood, D.R., Doria, G., Gagen, M.H., Siever, P.A., and Westgate, J.A., 2017, Middle Eocene CO_2 and climate reconstructed from the sedimentary fill of a subarctic kimberlite maar: Geology, v. 45, p. 619–622, https://doi.org/10.1130/G39002.1.

Woodward, F.I., 1987, Stomatal numbers are sensitive to increase in CO_2 from pre-industrial levels: Nature, v. 327, p. 617–618, https://doi.org/10.1038/327617a0.

Zachos, J.C., Pagani, M., Sloan, L., Thomas, E., and Billups, K., 2001, Trends, rhythms and aberrations in global climate 65 Ma to present: Science, v. 292, p. 686–693, https://doi.org/10.1126/science.1059412.

Zeebe, R.E., Westhold, T., Littler, K., and Zachos, J.C., 2016, Orbital forcing of the Paleocene and Eocene carbon cycle: Paleoceanography, v. 32, p. 440–465, https://doi.org/10.1002/2016PA003054.

Zhang, Y.G., Pagani, M., Liu, Z., Bohaty, S.M., and DeConto, R., 2013, A 40-million-year history of atmospheric CO_2: Philosophical Transactions of the Royal Society A: Mathematical, Physical and Engineering Sciences, v. 371, 20130096, https://doi.org/10.1098/rsta.2013.0096.

Printed in USA